Mutant K-*ras* Regulates Cathepsin B Localization on the Surface of Human Colorectal Carcinoma Cells[1]

Dora Cavallo-Medved, Julie Dosescu*, Bruce E. Linebaugh*, Mansoureh Sameni*, Debbie Rudy* and Bonnie F. Sloane*,†*

*Department of Pharmacology and †Barbara Ann Karmanos Cancer Institute, School of Medicine, Wayne State University, Detroit, MI 48201, USA

Abstract

Cathepsin B protein and activity are known to localize to the basal plasma membrane of colon carcinoma cells following the appearance of K-*ras* mutations. Using immunofluorescence and subcellular fractionation techniques and two human colon carcinoma cell lines—one with a mutated K-*ras* allele (HCT 116) and a daughter line in which the mutated allele has been disrupted (HKh-2)—we demonstrate that the localization of cathepsin B to caveolae on the surface of these carcinoma cells is regulated by mutant K-*ras*. In HCT 116 cells, a greater percentage of cathepsin B was distributed to the caveolae, and the secretion of cathepsin B and pericellular (membrane-associated and secreted) cathepsin B activity were greater than observed in HKh-2 cells. Previous studies established the light chain of annexin II tetramer, p11, as a binding site for cathepsin B on the surface of tumor cells. The deletion of active K-*ras* in HKh-2 cells reduced the steady-state levels of p11 and caveolin-1 and the distribution of p11 to caveolae. Based upon these results, we speculate that cathepsin B, a protease implicated in tumor progression, plays a functional role in initiating proteolytic cascades in caveolae as downstream components of this cascade (e.g., urokinase plasminogen activator and urokinase plasminogen activator receptor) are also present in HCT 116 caveolae.

Neoplasia (2003) **5**, 507–519

Keywords: Cancer, cysteine proteases, membrane-associated proteases, caveolae, K-*ras*.

Introduction

Malignant progression involves degradation of extracellular matrix (ECM) proteins at several steps (e.g., angiogenesis and the intravasation and extravasation of tumor cells during hematogenous metastasis) [1,2]. These invasive processes have long been known to be mediated by enzymatic cascades of multiple proteases and protease classes [3]. Cathepsin B, a lysosomal cysteine protease, is one of these enzymes [4]. Cathepsin B is synthesized as a preproenzyme and is activated in prelysosomal acidic vesicles (i.e., late endosomes) [5]. This enzyme exhibits both endopeptidase and exopeptidase activities, with the latter activity predominant at the acidic conditions found in lysosomes [6]. Cathepsin B can be stabilized by protein substrates and has been shown to degrade ECM proteins *in vitro* at both acidic and neutral pH [7]. Membrane-associated cathepsin B can be isolated from a variety of tumor cell lines [8,9] and membrane-associated cathepsin B activity can be assayed on living cells in culture (i.e., at neutral pH) [10]. Such observations suggest that cathepsin B may participate in proteolysis outside the cell. Indeed, Brix et al. [11] have shown that cathepsin B degrades cross-linked insoluble thyroglobulin in the lumen of thyroid follicles. Additional cysteine proteases and proteolytic cascades of cysteine proteases are also believed to be involved in the degradation of thyroglobulin and liberation of active thyroid hormones [11]. Using a confocal assay that we developed to image proteolysis by living cells, we have established that cathepsin B degrades type IV collagen at the surface of living cells from breast [12], colorectal [13], and prostate (Podgorski et al., unpublished observations) carcinomas and gliomas [14]. Our confocal assays implicate proteolytic cascades of more than one protease class [the cysteine protease cathepsin B, the serine proteases urokinase plasminogen activator (uPA) and plasmin(ogen), and matrix metalloproteinase (MMP)] in degradation of type IV collagen [12]. Cathepsin B has been shown by us and others to activate pro-uPA [15–17], resulting in increased invasion of ovarian carcinoma cells [15] and activation of latent transforming growth factor-β (TGF-β) [17]. During epithelial–mesenchymal transitions, TGF-β–stimulated ERK signaling regulates genes with functions in cell matrix

Abbreviations: AIIt, annexin II tetramer; AU, arbitrary unit; BCA, bicinchoninic acid; β-gal, β-galactosidase; CA-074, *N*-(L-3-*trans*-propyl-carbamoyloxirane-2-carbonyl)-L-isoleucyl-L-proline; DMEM, Dulbecco's minimal essential medium; ECM, extracellular matrix; FBS, fetal bovine serum; LAMP-1, lysosomal-associated membrane protein-1; MES, 2-[*N*-morpholino] ethanesulfonic acid; PAGE, polyacrylamide gel electrophoresis; PBS, phosphate-buffered saline; PIPES, piperazin-*N*-*N* -bis[2-ethanesulfonic acid]; SDS, sodium dodecyl sulfate; TBS, Tris-buffered saline; TGF-β, transforming growth factor-β; tPA, tissue plasminogen activator; uPA, urokinase plasminogen activator; uPAR, urokinase plasminogen activator; UPAR, urokinase receptor; Z-Arg-Arg-NHMec, benzyloxycarbonyl-L-arginyl-L-arginine-4-methyl-7-coumarylamide

Address all correspondence to: Bonnie F. Sloane, Department of Pharmacology, Wayne State University, 540 East Canfield, Detroit, MI 48201, USA. E-mail: bsloane@med.wayne.edu

[1]This work was supported by the National Institutes of Health (NIH) grant 56586. The Microscopy and Imaging Resources Laboratory is supported, in part, by NIH Center grants P30ES06639 and P30ES22453. D.C.-M. was supported by a Natural Sciences and Engineering Research Council of Canada Postdoctoral Fellowship.

Received 13 August 2003; Revised 25 September 2003; Accepted 26 September 2003.

adhesion, cell motility, and endocytosis including several MMP and ECM components [18]. Elevated TGF-β1 levels in colon carcinoma cells stimulate cell growth—a process that is dependent on the mutation of K-*ras* [19].

In colorectal carcinomas, high levels of cathepsin B expression are predictive of shorter overall survival [20]. In parallel with malignant progression to late adenomas and early carcinomas, cathepsin B moves from the apical region of the cells to the basal plasma membranes [20]. The mechanism by which cathepsin B becomes associated with the basal plasma membrane remains to be elucidated; however, the basal enzyme is active [21]. The association of cathepsin B with the basal plasma membrane occurs in late adenomas and thus coincides with the activation of K-*ras* [22]. This is intriguing as cathepsin B has also been shown to move to the surface of breast epithelial cells that have been transfected with activated c-H-*ras* [23]. Nonetheless, increases in expression of cathepsin B and translocation of active cathepsin B to the basal membrane are also observed during the progression of adenomas in Min mice [24], a model for familial adenomatous polyposis in humans that is not associated with alterations in K-*ras* (for review, see Ref. [25]). The membrane association of cathepsin B, the upregulation of caveolin-1 in colon cancer, and the association of activated K-*ras* with colon cancer progression [22] led us to use two human colorectal carcinoma cell lines that differ in their expression of mutant K-*ras* [26] to evaluate potential interactions among activated ras, cathepsin B, and caveolin-1. Analysis of these cell lines was also of interest due to the controversy in the literature as to "which *ras* rides the [lipid] raft" [27]. The cell surface receptor for the serine protease uPA, urokinase plasminogen activator receptor (uPAR), has been localized to caveolae [28] as have MT1-MMP [29,30] and MMP-2 [30]. Also found in the caveolae is annexin II tetramer (AIIt) [31,32], a potential binding protein for such proteases as tissue plasminogen activator (tPA) and plasmin(ogen) (for review, see Ref. [33]), and procathepsin B [34]. We demonstrate that active cathepsin B localizes to the caveolae region of colon cancer cells and that uPA, uPAR, and AIIt are also associated with caveolae in these cells. On this basis, we hypothesize that one function of caveolae is to cluster proteases on the cell surface, thereby facilitating initiation of proteolytic cascades. Furthermore, we show reduced expression of caveolin-1, the light chain of AIIt (p11), and pericellular cathepsin B activity in the colorectal carcinoma cell line in which K-*ras* has been disrupted (i.e., in the less malignant HKh-2 daughter cell line) [26,35].

Materials and Methods

Reagents

The human colorectal carcinoma cell lines HCT 116 and HKh-2 were kind gifts from Dr. Robert Kerbel (Sunnybrook Health Science Center, Toronto, Canada) and Dr. Takehiko Sasazuki (Kyushu University, Higashi, Japan). Dulbecco's minimal essential medium (DMEM), Hank's salt solution, bovine serum albumin (BSA), antibiotics, glutamine, saponin, octylglucoside, 2-[*N*-morpholino]ethanesulfonic acid (MES), calf thymus DNA, heparin, bisbenzimide dye H-33258, and all other chemicals, unless otherwise stated, were from Sigma (St. Louis, MO); fetal bovine serum (FBS) was from Invitrogen Life Technologies, Carlsbad, CA; anti–caveolin polyclonal antibodies, monoclonal anti-p36 (mAb 5), and monoclonal anti-p11 (mAb 148) antibodies were purchased from Transduction Laboratories (Lexington, KY); rabbit anti–cathepsin B antibodies were produced and characterized in our laboratory [36]; monoclonal anti–lysosomal-associated membrane protein-1 (LAMP-1) (H4A3) antibodies were from the Developmental Studies Hybridoma Bank (University of Iowa, Iowa City, IA); polyclonal anti–β-galactosidase (β-gal) antibodies were from Chemicon Technical Services (Temecula, CA); polyclonal anti-uPA and polyclonal anti-uPAR antibodies were a kind gift from Dr. Gunilla Hoyer-Hansen (The Finsen Center, Copenhagen, Denmark); horseradish peroxidase–labeled goat anti–rabbit and goat anti–mouse IgG and micro-bicinchoninic acid (BCA) reagents were from Pierce (Rockford, IL); fluorescein-conjugated affinity-purified donkey anti–rabbit IgG, Texas red–conjugated affinity-purified donkey anti–mouse IgG, and normal donkey serum were from Jackson ImmunoResearch (West Grove, PA); SlowFade antifade reagent was from Molecular Probes (Eugene, OR); acrylamide and nitrocellulose membranes were from BioRad (Hercules, CA); prestained protein markers and chemiluminescent Western blotting detection kits were from Amersham Pharmacia Biotech (Piscataway, NJ); protease inhibitors were from Roche Molecular Biochemicals (Indianapolis, IN); benzyloxycarbonyl-L-arginyl-L-arginine-4-methyl-7-coumarylamide (Z-Arg-Arg-NHMec) was from Bachem (Torrance, CA); and the cathepsin B inhibitor, *N*-(L-3-*trans*-propyl-carbamoyloxirane-2-carbonyl)-L-isoleucyl-L-proline (CA-074), was from Peptides International (Louisville, KY).

Cell Culture

HCT 116 and HKh-2 cells were grown in DMEM (low glucose) with glutamine, supplemented with antibiotics (penicillin/streptomycin) and 10% (vol/vol) FBS in 5% CO_2/humidifed atmosphere at 37°C. Experiments were carried out when cells were approximately 80% confluent.

Preparation of Caveolae-Enriched Membrane Fractions

Preparation of caveolae-enriched membrane fractions was performed as previously described [37,38]. Briefly, cells from 6 × 100-mm dishes were washed twice with phosphate-buffered saline (PBS) and then scraped into 2 ml of 500 mM sodium carbonate, pH 11.0. Cells were homogenized by 10 strokes in a loose-fitting Dounce homogenizer. The lysates were then sonicated on ice in a 50-W Ultrasonicator at 3 × 20 second pulses and adjusted to equal protein concentrations. The homogenates were adjusted to 45% sucrose by the addition of 2 ml of 90% (wt/vol) sucrose prepared in MES-buffered saline (25 mM MES, pH 6.5, 0.15 m NaCl) and placed on the bottom of a 12-ml ultracentrifuge tube. The homogenate was overlaid with a 5% to 35% discontinuous gradient by adding 4 ml of 35% (wt/vol)

sucrose (in MES-buffered saline containing 250 mM sodium carbonate) and 4 ml of 5% (wt/vol) sucrose (in MES-buffered saline containing 250 mM sodium carbonate) and centrifuged at 39,000 rpm for 18 to 20 hours in a SW41 rotor (Beckman Instruments, Fullerton, CA) at 4°C. A light scattering band was observed at the 5% to 35% sucrose interface. From the top of the gradient, 1-ml fractions were collected to yield a total of 12 fractions. Equal volume aliquots from each gradient fraction were analyzed by sodium dodecyl sulfate polyacrylamide gel electrophoresis (SDS-PAGE) and immunoblotting.

Preparation of Cellular Extracts

Cells were washed twice with PBS and solubilized in lysis buffer (10 mM Tris, pH 7.5, 50 mM NaCl, 1% Triton X-100, 60 mM octylglucoside, 0.1 mM aprotinin, and 1 mM leupeptin). In the analysis of cathepsin B, cells were solubilized in a lysis buffer containing 250 mM sucrose, 25 mM MES, pH 7.5, 1 mM EDTA plus 0.1% Triton X-100. Cell extracts were then passed 10 times through a syringe with a 20-gauge needle and centrifuged for 5 minutes at 10,000*g*. The cell homogenate supernatant was recovered and protein concentrations were quantified using micro-BCA reagents according to the manufacturer's instructions. Equal protein aliquots of each sample were analyzed by SDS-PAGE and immunoblotting.

SDS-PAGE and Immunoblot Analysis

Samples were separated by SDS-PAGE (7%, 12%, or 15% acrylamide) and transferred to nitrocellulose membranes. Immunoblotting was performed with primary antibodies against cathepsin B (1:4000), caveolin (1:5000), p36 (1:5000), p11 (1:5000), LAMP-1 (1:500), β-gal (1:4000), uPA (5 μg/ml), uPAR (5 μg/ml), and secondary antibodies conjugated with horseradish peroxidase (1:10,000) in Tris-buffered saline (TBS) wash buffer (20 mM Tris, pH 7.5, 0.5 M NaCl) containing 0.5% Tween 20 and 5% (wt/vol) nonfat dry milk. We should indicate that although the rabbit anti–β-gal polyclonal antibody was raised against bacterial β-gal, this antibody also cross-reacts with the human homologue (Chemicon Technical Services). We confirmed this prior to using this antibody for these studies (data not shown). After washing, specifically bound antibodies were detected by enhanced chemiluminescence according to the manufacturer's instructions. Quantitation and analysis of bands were performed using a Luminescent Image Analyzer LAS-1000 Plus (Fujifilm, Stamford, CT) and expressed as arbitrary units (AU) per square millimeter. Statistical significance was determined by a two-tailed *t*-test with assumed equal variance. * represents a *P* value less than .05 and ** represents a *P* value less than .01.

Immunocytochemical Staining and Confocal Microscopy

Cells were grown on glass coverslips to 80% confluency, and either used for intracellular or surface staining as previously described [12,39]. Surface staining was carried out at 4°C using nonpermeabilized cells, whereas intracellular staining was carried out at room temperature using saponin-permeabilized cells. For surface staining, the primary antibodies used were rabbit anti–human liver cathepsin B (5 μg/ml) and mouse anti–human p11 (20 μg/ml), and for intracellular staining, the antibodies used were rabbit anti–human caveolin (5 μg/ml) and mouse anti–human p11 (20 μg/ml). Secondary antibodies used were fluorescein-conjugated affinity-purified donkey anti–rabbit IgG and Texas red–conjugated affinity-purified donkey anti–mouse IgG (20 μg/ml). Coverslips were mounted upside down with SlowFade antifade reagent on glass slides and the cells were observed on a Zeiss LSM 310 microscope (Jena, Germany) in confocal mode.

Continuous "Real-Time" Cathepsin B Activity Assay

Cathepsin B activity assays on living cells were performed by the methods described in Linebaugh et al. [10]. Briefly, cells were grown on 9 × 22-cm coverslips to 80% confluency and washed in PBS containing 1.0 mM $CaCl_2$ and 0.5 mM $MgCl_2$, pH 7.4, at 37°C. Cells were then incubated in "real-time" assay buffer [Hank's balanced salt solution lacking sodium bicarbonate and containing 0.6 mM $CaCl_2$, 0.6 mM $MgCl_2$, 2 mM L-cysteine, 10 mM glucose, and 25 mM piperazin-*N*-*N*′-bis[2-ethanesulfonic acid] (PIPES) (disodium salt), pH 7.0] and 100 μM Z-Arg-Arg-NHMec substrate for 15 minutes at 37°C. During this time period, cathepsin B activity was measured in a Shimadzu RF-540 spectrofluorophotometer (Columbia, MD) at an excitation of 380 nm and emission of 460 nm as the rate of fluorescent product (7-amino-4-methylcoumarin) formation. This activity represented pericellular cathepsin B activity and included both membrane-bound and secreted activities. To measure total cellular cathepsin B activity, cells in the reaction cuvette were further treated with 0.1% Triton X-100 and activity was measured for an additional 5 minutes. The highly selective cathepsin B inhibitor, CA-074 [40], was then added to all reactions at a final concentration of 10 mM to confirm that cathepsin B was responsible for the enzymatic activity observed during the reaction. Specific activity for cathepsin B was calculated as picomoles of fluorescent product per minute per microgram of DNA. Statistical significance was determined by a two-tailed *t*-test with assumed equal variance. * represents a *P* value less than .05 and ** represents a *P* value less than .01.

DNA Assay

Coverslips containing whole cells from "real-time" assays were stored in 2 × DNA assay buffer (200 mM NaCl, 20 mM EDTA, 20 mM Tris, pH 7.0), freeze-thawed, and sonicated for 2 × 10 second pulses. Then 50 μl of cell lysate was added to 1.0 ml of bisbenzimide solution (one part H_2O, 0.001 part 200 mg/ml bisbenzimide dye H-33258, and one part 2 × DNA assay buffer) and incubated at room temperature in the absence of light for 10 minutes. Fluorescence was measured in a Shimadzu RF-540 spectrofluorophotometer at an excitation of 350 nm and emission of 455 nm. Relative fluorescence was plotted against a standard DNA

curve from calf thymus DNA to determine the concentration of DNA per sample.

Results

Active K-ras Is Associated with Increased Secretion and Pericellular Activity of Cathepsin B in Human Colorectal Carcinoma Cell Lines

The colorectal carcinoma cell lines used for these studies were parental HCT 116 cells, which contain a point mutation that activates one of the K-*ras* alleles, and HKh-2 cells, a subline disrupted at the activated allele [26]. The less tumorigenic HKh-2 cells grow more slowly both *in vitro* and *in vivo* [26] and exhibit 80% less degradation of the basement membrane protein laminin than do HCT 116 cells [35]. Our initial studies compared the steady-state level of cathepsin B in these two cell lines. Intracellular cathepsin B was found predominantly as the two active forms of cathepsin B: the mature single-chain (31 kDa) isoform and the heavy chain (25/26 kDa) of the mature double-chain isoform. Interestingly, the expression of active double-chain cathepsin B was significantly greater in HKh-2 cells than in HCT 116 cells (Figure 1*A*). Inactive procathepsin B (43/46 kDa) was not detected intracellularly in either cell line (data not shown). Instead, procathepsin B, along with both isoforms of mature cathepsin B, was secreted from both cell lines (Figure 1*A*), with HCT 116 cells secreting higher levels of cathepsin B than HKh-2 cells. Thus, these data suggest that mutated K-*ras* may contribute to the altered distribution and increased secretion of cathepsin B observed in HCT 116 cells.

The difference in distribution of cathepsin B between the two cell lines was further demonstrated by using a "real-time" continuous assay for cathepsin B activity. This "real-time" assay measures the rate of Z-Arg-Arg-NHMec hydrolysis by living cells grown on coverslips [10]. Cathepsin B activity could be measured in both colon carcinoma cell lines; however, the percentage of cathepsin B activity that was pericellular (membrane-associated plus secreted) was significantly greater (approximately three-fold) in the HCT 116 cells than in the HKh-2 cells (Figure 1*B*). Along with observations made in Figure 1*A*, these data suggest a role for K-*ras* in the distribution of active cathepsin B on both the surface of these colon cancer cells and in their extracellular milieu.

Cathepsin B Associates with AIIt on the Surface of Human Colorectal Carcinoma Cell Lines

Our previous studies using both breast carcinoma and glioma cells demonstrate that cathepsin B associates with the plasma membrane through interactions with p11, the light chain of AIIt [34]. The AIIt is composed of two light chains (p11) and two heavy chains (p36). p11 appears to mediate the interaction of AIIt with the plasma membrane, and p36 is thought to function as a cell surface receptor to several proteins (for review, see Ref. [41]). To determine whether K-*ras* modulates the expression of AIIt, we compared the intracellular steady-state levels of p11 and p36 in HCT 116 and HKh-2 cells. Although both cell lines expressed p11 and p36, HKh-2 cells expressed less p11 (~50%) than did HCT 116 cells (Figure 2*A*). In contrast, the intracellular steady-state levels of p36 were comparable between the two cell lines (Figure 2*A*). These results suggest a role for K-*ras* in the expression of p11 that may contribute to altered distribution of cathepsin B in HCT 116 cells.

In our previous studies, the association between cathepsin B and p11 was revealed using several techniques, including interaction of recombinant proteins *in vitro*, coimmunoprecipitation from tumor cell membranes with an antibody to the annexin II heavy-chain p36, and colocalization on the tumor cell surface by immunofluorescent surface staining [34]. Here we used the same surface staining procedure to illustrate the association of cathepsin B with p11 in HCT 116 cells. HCT 116 cells were chosen to demonstrate this association due to their higher level of expression of p11 protein. For these studies. we used an established protocol for staining of surface proteins [39,12] that does not permeabilize cells and thus allows one to differentiate cell surface cathepsin B from lysosomal cathepsin B. The anti–cathepsin B antibody recognizes both procathepsin B and the active single-chain and double-chain forms of the enzymes [36], and thus would not discriminate among the molecular forms of cathepsin B but would establish that cathepsin B was present on the cell surface. In HCT 116 cells, surface staining for cathepsin B and p11 was observed as discrete green and red patches, respectively, on the cell surface (Figure 2*B*), a pattern similar to that observed for cathepsin B and p11 on the surface of BT20 human breast carcinoma and U87 human glioma cells [34] and for p11 on human HT1080 fibrosarcoma [42] and human umbilical vein endothelial cells [43]. The areas of overlap for cathepsin B and p11 staining on the surface of HCT 116 cells appear yellow (Figure 2*B*). Not all cells exhibit surface staining for either cathepsin B or p11 as also observed in previous studies by us [34] and others [42,43]. Although the fluorescent images for cathepsin B and p11 do not verify a direct interaction between cathepsin B and p11, they do establish that the two proteins are present in close proximity on the surface of HCT 116 tumor cells.

AIIt Associates with Caveolae of Human Colorectal Carcinoma Cell Lines

Previous studies have localized AIIt to caveolae of endothelial and MDCK cells [31,32]. Here we explored the effects of K-*ras* on the association of p11 and p36 with caveolae in the HCT 116 and HKh-2 cells. Because the levels of p11 in HCT 116 cells were higher than in HKh-2 cells (cf. Figure 2*A*), we analyzed the expression of caveolin-1, a major structural protein of caveolae, in both HCT 116 and HKh-2 cells. Both cell lines expressed caveolin-1, but the steady-state level of caveolin-1 in HKh-2 cells was ~25% lower than HCT 116 cells (Figure 3*A*).

To isolate caveolae and their associated proteins from colon carcinoma cells, we employed a well-established protocol [37] based on the insolubility of caveolae to carbonate extraction and their specific buoyant density in

equilibrium sucrose gradients. This procedure separates caveolae and their associated proteins from > 99.95% of the total cellular proteins including organelle-specific markers for endoplasmic reticulum, Golgi, lysosomes, mitochondria, and noncaveolae membranes [31,44,45]. Fractionation of HCT 116 and HKh-2 cells established that the bulk of caveolin-1 (seen as α and β isoforms) was isolated in low-density fractions 3 to 6, hereafter designated as caveolae fractions (Figure 3*B*). The polyclonal caveolin antibody used in this study is a general caveolin antibody; however, we have verified the presence of caveolin-1 in these cells using a monoclonal caveolin-1 antibody (mAb C060; Transduction Laboratories, Lexington, KY) (data not shown). In both cell lines, fractionation studies revealed that p36, the annexin II heavy chain, was present in caveolae fractions and in the high-density fractions 7 to 12, hereafter

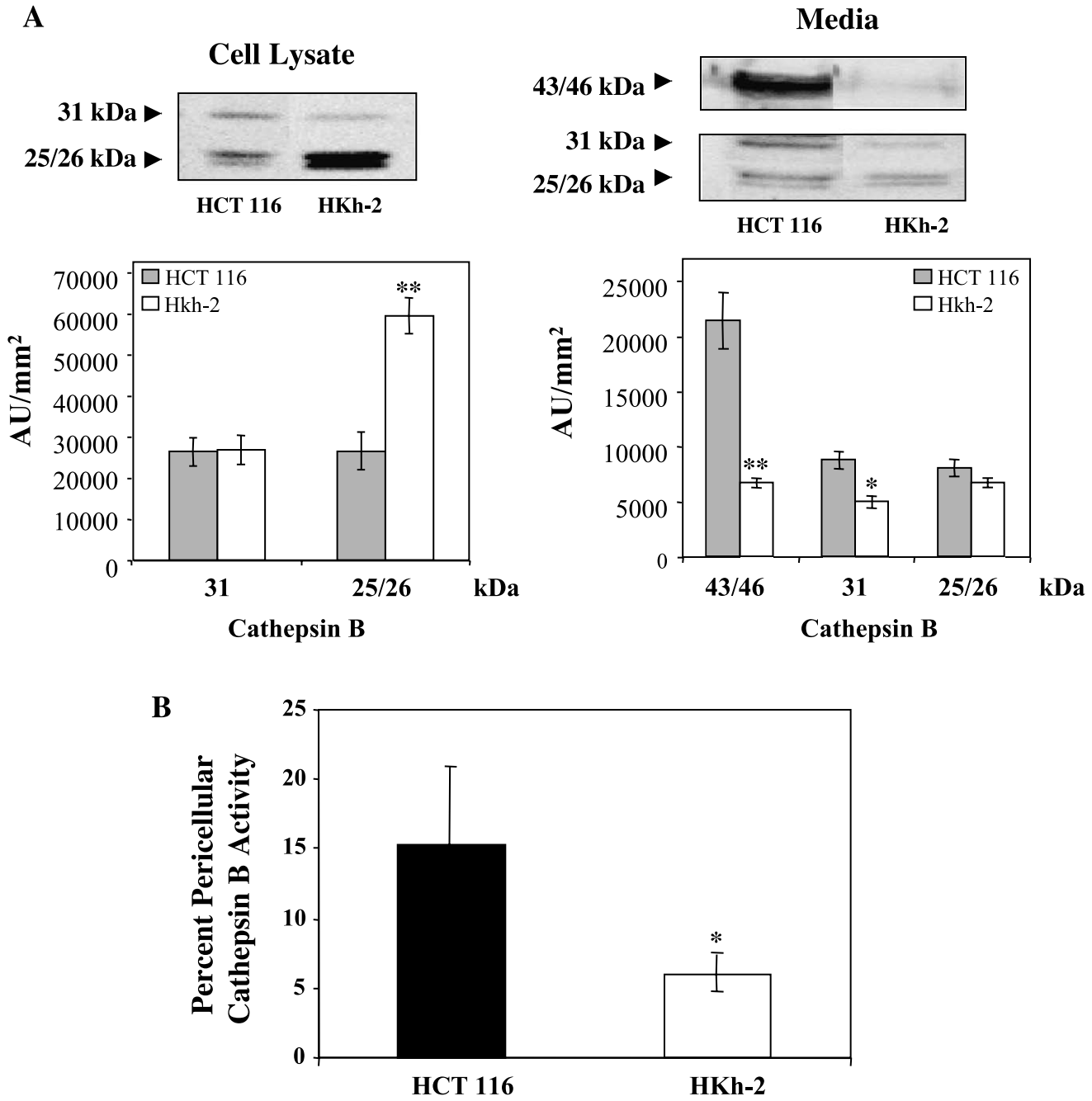

Figure 1. *Differences in the expression, secretion, and activity of cathepsin B in HCT 116 and HKh-2 cells. (A) Conditioned media from HCT 116 and HKh-2 cells were collected and the cells were solubilized in lysis buffer containing 0.1% Triton X-100. Media and cell lysates (40 μg of protein) were analyzed by SDS-PAGE and immunoblotted with anti–human cathepsin B antibody. Bar graphs represent densitometric analysis of protein bands from at least three experiments (expressed as AU/mm^2); mean ± SD. *P < .05, **P < .01. (B) HCT 116 and HKh-2 cells were grown on glass coverslips to 80% confluency. The pericellular (membrane-associated and secreted) and total cathepsin B activities in these living cells were measured against Z-Arg-Arg-NHMec substrate (see Materials and Methods section). Reactions were terminated by the addition of 10 μM of the cathepsin B-selective inhibitor, CA-074 [40]. The specific activity for pericellular cathepsin B was expressed as a percent of the total cathepsin B activity in HCT 116 and HKh-2 cells. The graph is representative of at least three experiments and presented as mean ± SD. *P < .05.*

designated as noncaveolae fractions (Figure 3*B*). p11, the annexin II light chain, was present in noncaveolae fractions of both cell lines and in caveolae fractions of HCT 116 cells, but could not be detected in caveolae fractions of HKh-2 daughter cells (Figure 3*B*). These results suggest that active K-ras affects the expression of caveolin-1 and p11 as well as the distribution of p11 to caveolae fractions in HCT 116 cells.

Double labeling of saponin-permeabilized HCT 116 cells was performed to further establish an association between caveolin-1 and p11 in these cells. Permeabilization of HCT 116 cells is required because the caveolin-1 antibody is

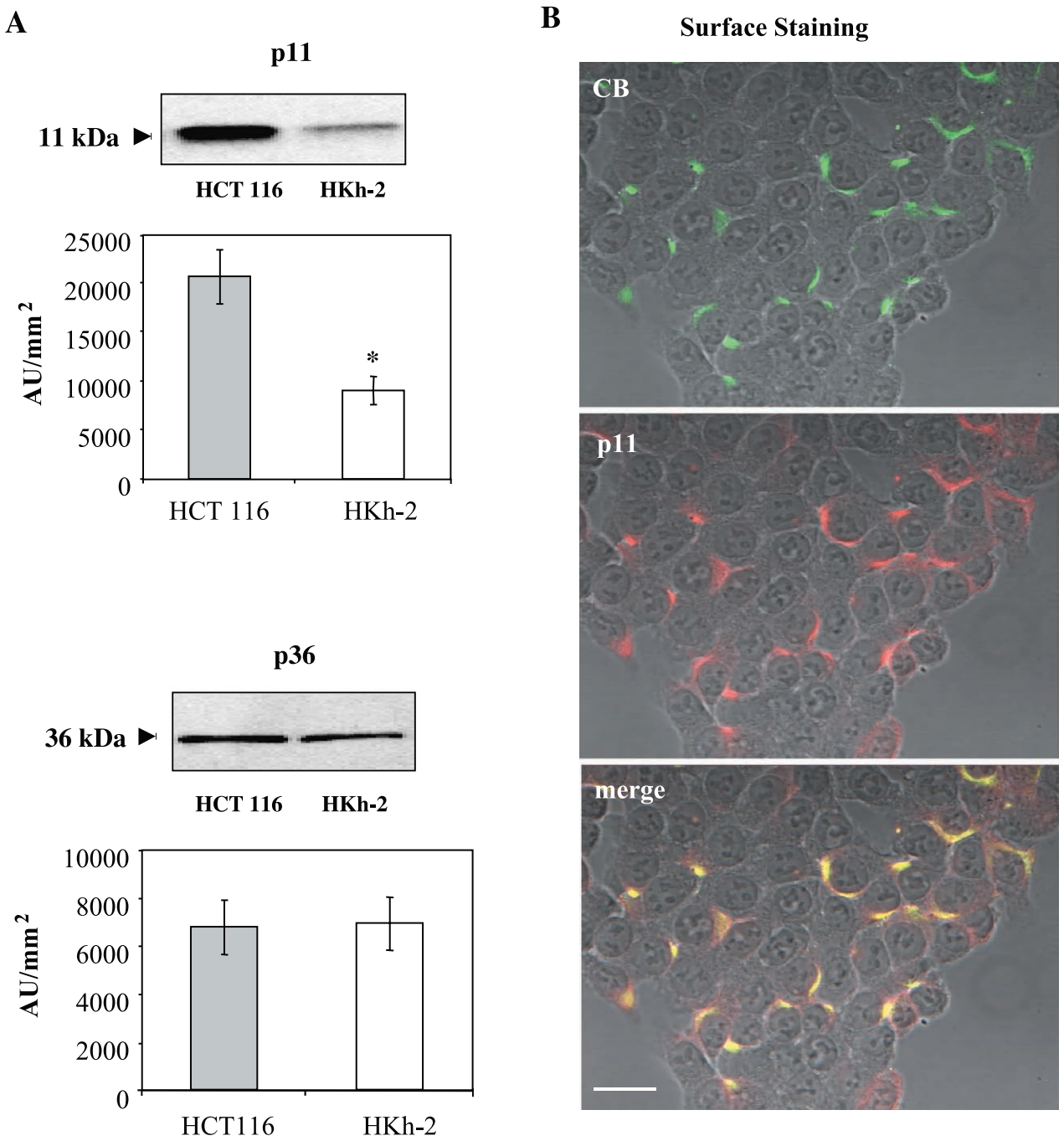

Figure 2. *Expression of AIIt and its association with cathepsin B in human colorectal carcinoma cells. (A) HCT 116 and HKh-2 cells were solubilized in lysis buffer containing 1% Triton X-100 and 60 mM octylglucoside. Ten milligrams of protein was analyzed by SDS-PAGE and immunoblotted with anti–human p11 and anti–human p36 antibodies. Bar graphs represent densitometric analysis of protein bands from at least three experiments (expressed as AU/mm^2); mean ± SD. *P < .05, **P < .01. (B) Surface staining was performed on HCT 116 cells grown on glass coverslips as described in Materials and Methods section. Cells were incubated in the absence of detergents with primary antibodies, monoclonal anti–human p11 IgG, plus rabbit anti–human cathepsin B IgG. Cells were then incubated with FITC-conjugated affinity-purified donkey anti–rabbit and Texas red–conjugated affinity-purified donkey anti–mouse IgG plus normal donkey serum. The cells were observed with a Zeiss LSM 310 microscope in confocal mode at a magnification of × 630 under oil immersion. Surface immunostaining for cathepsin B and p11 is shown in green and red, respectively. Areas of overlap for cathepsin B and p11 staining are shown in yellow on the cell surface. These images are representative of three experiments. Bar, 20 μm.*

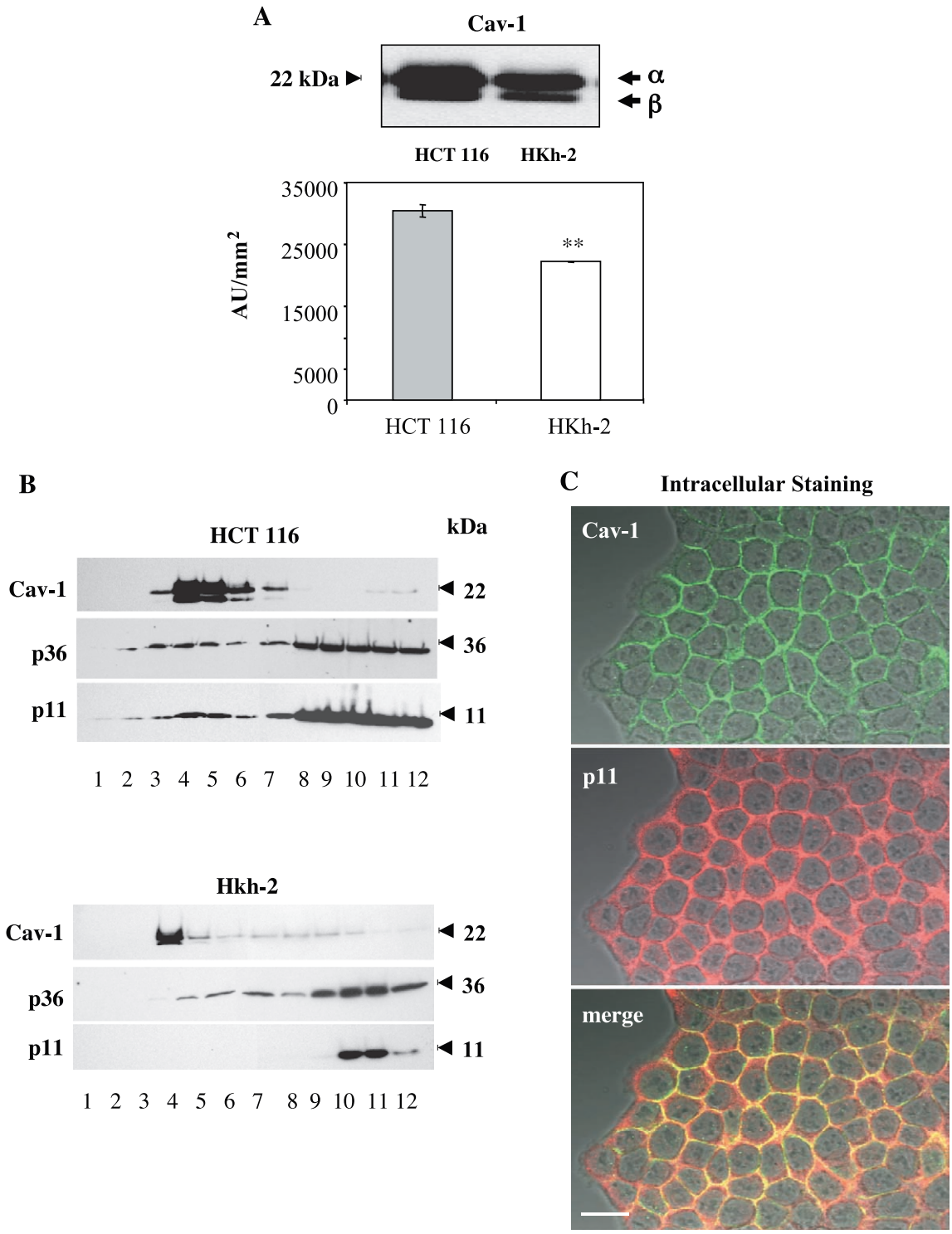

Figure 3. *Expression of caveolin-1 and its association with AIIt in human colorectal carcinoma cells. (A) HCT 116 and HKh-2 cells were solubilized in lysis buffer containing 1% Triton X-100 and 60 mM octylglucoside. Ten micrograms of protein was analyzed by SDS-PAGE and immunoblotted with anti–human caveolin-1. Bar graphs represent densitometric analysis of protein bands from at least three experiments (expressed as AU/mm^2); mean ± SD. *P < .05, **P < .01. (B) Equal amounts of protein for HCT 116 and HKh-2 cells were subjected to subcellular fractionation on a sucrose gradient after homogenization in sodium carbonate buffer, pH 11.0 (see Materials and Methods section). Fractions were collected from the top of the gradient and equal volume aliquots were analyzed by SDS-PAGE and immunoblotting. Panels from top to bottom represent fractions from HCT 116 and HKh-2 cells probed with rabbit anti–human caveolin-1 (top), mouse anti–human p36 (middle), and mouse anti–human p11 (bottom). These are representative of at least three experiments. (C) Intracellular staining was performed on HCT 116 cells grown on glass coverslips, as described in Materials and Methods section. Cells were incubated in the presence of saponin with primary antibodies, monoclonal anti–human p11 IgG, plus rabbit anti–human caveolin-1 IgG. Cells were then incubated with FITC-conjugated affinity-purified donkey anti–rabbit and Texas red–conjugated affinity-purified donkey anti–mouse IgG plus normal donkey serum. The cells were observed with a Zeiss LSM 310 microscope in confocal mode at a magnification of × 630 under oil immersion. Intracellular immunostaining for caveolin-1 and p11 is shown in green and red, respectively. Areas of overlap for caveolin-1 and p11 staining are shown in yellow adjacent to the cytoplasmic face of the cell membrane. These images are representative of three experiments. Bar, 20 μm.*

directed to the N-terminal cytoplasmic tail of the protein (Transduction Laboratories). Staining for caveolin-1 could be observed as a discrete green ring adjacent to the cell membrane (Figure 3*C*). p11 is an intracellular protein as well as a caveolar protein, and thus staining for p11 should be present as red fluorescence throughout the cytoplasm of the HCT 116 cells. This was indeed the observed pattern of staining for p11. The HCT 116 cells are small and have large nuclei, so the extent of intracellular staining for p11 (Figure 3*C*) can best be appreciated by comparing it with the surface staining for p11 in nonpermeabilized cells (cf. Figure 2*B*). The areas of overlap for caveolin-1 and p11 staining in HCT 116 cells appear as a discrete yellow ring adjacent to the cell membrane (Figure 3*C*). Additional staining representing only p11 can be distinguished as red fluorescence in many cells. Although these fluorescent images do not verify a direct interaction between caveolin-1 and p11, they do establish that the two proteins are present in close proximity to the inner cell membrane of the HCT 116 cells.

Cathepsin B Associates with Caveolae of Human Colorectal Carcinoma Cell Lines

Because p11 was present in caveolae of HCT 116 cells, we analyzed these subcellular fractions for cathepsin B. In these sucrose density gradients, cathepsin B was distributed in two populations: one in caveolae fractions and another in denser noncaveolae fractions (Figure 4*A*). The predominant forms of cathepsin B in both populations were the heavy chain (25/26 kDa) of the double-chain form and the 31-kDa single-chain form. The presence of active cathepsin B in caveolae fractions of colon cancer cells indicates that this enzyme could participate in cell surface proteolytic events. As a comparison, we also analyzed the subcellular fractions of HKh-2 cells and found cathepsin B in both caveolae and noncaveolae fractions. Quantitation of the amount of cathepsin B in each fraction as a percent of the total cathepsin B revealed that the level of cathepsin B in caveolae fractions of HCT 116 cells was substantially greater than in caveolae fractions of HKh-2 cells (Figure 4*B*). Cathepsin B in HKh-2 cells was predominantly localized to noncaveolae fractions that include lysosomes, whereas in HCT 116 cells, cathepsin B was comparably distributed in caveolae and noncaveolae fractions. These data suggest that the activation of K-*ras* may alter pathways for the trafficking of cathepsin B to caveolae.

Cathepsin B is a lysosomal protease; however, in tumor cells, cathepsin B is also secreted and becomes associated with the cell surface [4]. To confirm that the presence of cathepsin B in caveolae fractions isolated from colon cancer cells was not due to lysosomal contamination during the isolation procedure, we examined the distribution of an insoluble lysosomal marker protein, LAMP-1, and a soluble lysosomal marker protein, β-gal, in the subcellular fractions of HCT 116 cells. We then compared the distribution patterns for LAMP-1 and β-gal to those for caveolin-1 and cathepsin B (cf. Figure 4*A*). The peak for caveolin-1 was in fractions 3 to 6, whereas the peaks for the two lysosomal marker proteins, LAMP-1 and β-gal, were in fractions 7 to 11 (Figure 5). Cathepsin B was distributed bimodally with one peak in fractions 2 to 6 and another in fractions 7 to 11, confirming that the presence of cathepsin B in caveolae fractions was not due to cross-contamination of these fractions with lysosomes during the isolation procedure.

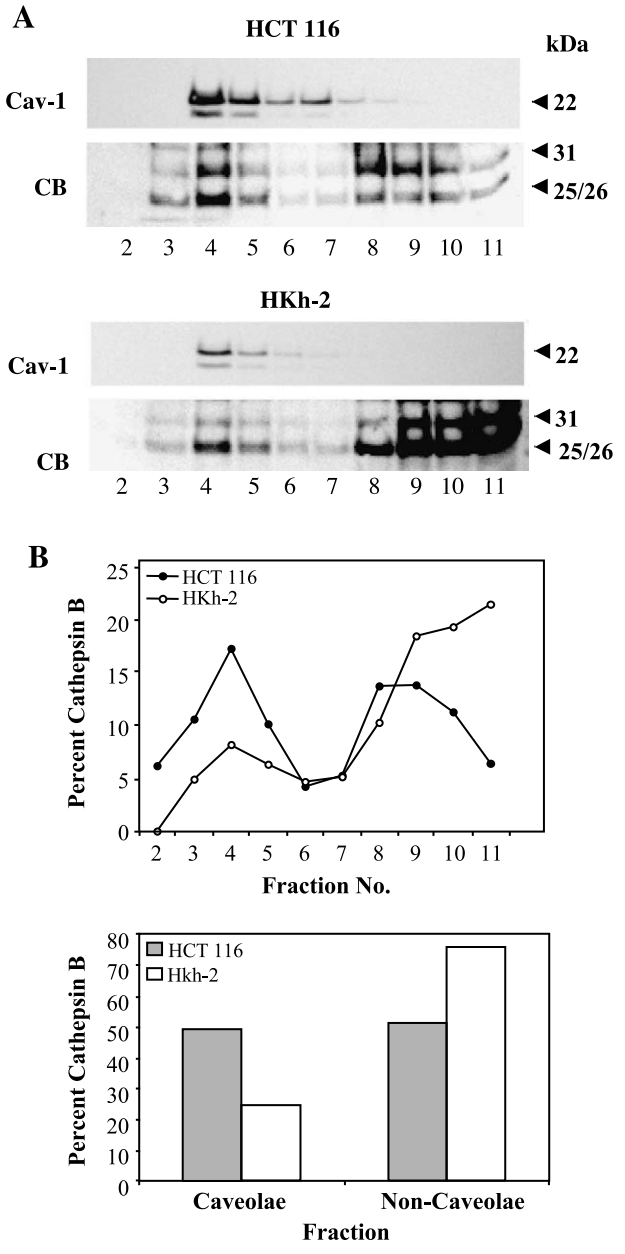

Figure 4. *Identification of cathepsin B in caveolae of human colorectal carcinoma cells. (A) Equal amounts of protein for HCT 116 and HKh-2 cells were subjected to subcellular fractionation on a sucrose gradient after homogenization in sodium carbonate buffer, pH 11.0 (see Materials and Methods section). Fractions were collected from the top of the gradient and equal volume aliquots were analyzed by SDS-PAGE and immunoblotting. Panels from top to bottom represent fractions 2 to 11 from HCT 116 and HKh-2 cells probed with rabbit anti-human caveolin-1 (top) and rabbit anti–human cathepsin B (bottom). These are representative of at least three experiments. (B) Densitometric analysis of the cathepsin B protein bands (31 + 25/26 kDa isoforms) from HCT 116 and HKh-2 fractions in (A) was performed and presented as percent cathepsin B in individual fractions as a function of the total (sum of fractions 2–11) and percent cathepsin B distributed into two major fractions: caveolae (sum of fractions 2–6) and noncaveolae (sum of fractions 7–11).*

uPA and uPAR Associate with Caveolae of HCT 116 Colorectal Carcinoma Cells

A potential role for active cathepsin B in caveolae is the initiation of proteolytic cascades via activation of pro-uPA [5,16,17]. uPAR, the receptor for both active uPA and pro-uPA, has been shown to complex with integrins and caveolin in tumor cells [28,46] and has been localized to caveolae of human chondrocytes [47]. uPAR has previously been detected in HCT 116 and HKh-2 cells and found to be expressed at levels 50% to 85% lower in HKh-2 cells [35]. Downregulation of uPAR in HKh-2 cells has been shown to result in the loss of surface uPA/uPAR–dependent activation of plasminogen [35]. We fractionated both HCT 116 and HKh-2 cells and analyzed the fractions for uPAR (Figure 6*A*) and uPA (Figure 6*B*). Both uPAR and uPA were present in caveolae fractions of HCT 116 cells and in noncaveolae fractions, as neither protein is exclusive to caveolae. Quantitation of the fractions revealed that the percent distribution of uPAR between caveolae and noncaveolae fractions was similar in both HCT 116 and HKh-2 cells (Figure 6*A*). The amount of uPAR is, however, substantially less in HKh-2 cells as also shown by others [35]. In contrast, quantitation of uPA revealed that the amount of uPA in the caveolae fractions as a percent of the total uPA was dramatically greater in HCT 116 cells compared to HKh-2 cells. Interestingly, the uPA distribution pattern between caveolae and noncaveolae fractions in HCT 116 and HKh-2 cells closely resembled that observed for cathepsin B in these cells (cf. Figure 4*B*). These data suggest that K-*ras* may also affect the trafficking of uPA to caveolae of these colon cancer cells.

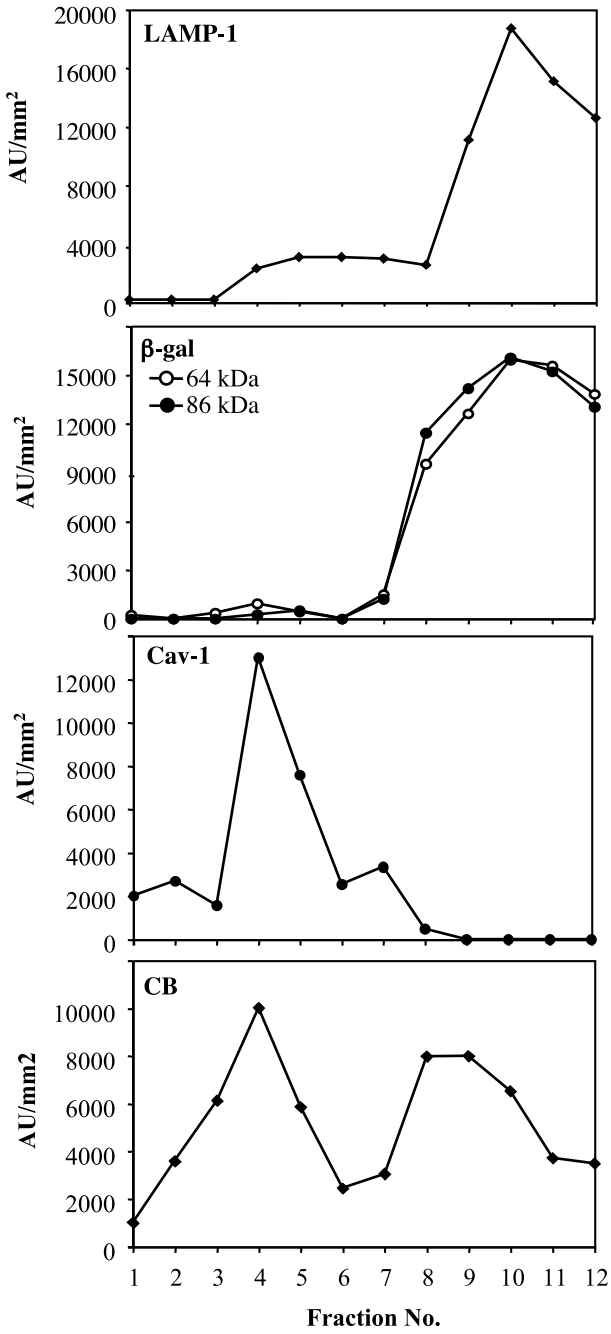

Figure 5. *Distribution of LAMP-1, β-gal, caveolin-1, and cathepsin B in sucrose gradient fractions of HCT 116 cells. Equal volume aliquots of HCT 116 sucrose gradient fractions illustrated in Figure 4A were subjected to SDS-PAGE; immunoblotted for LAMP-1, β-gal, caveolin-1, and cathepsin B; and the protein bands were analyzed by densitometry. The graphs represent the distribution of these proteins within the sucrose gradient fractions (expressed as AU/mm²).*

Discussion

Upregulation of cathepsin B expression and activity and redistribution of cathepsin B to the cell surface are typical characteristics observed in tumor cells (for review, see Ref. [48]). A correlation between the expression and activity of cell surface cathepsin B and the hydrolysis of ECM proteins has also been revealed. Thus, altered trafficking of cathepsin B to the plasma membrane of tumor cells implies a functional role for this enzyme in tumor invasion. Although cathepsin B has been detected on the surface of many human carcinomas, in the present study, we identify caveolae as sites for association of active cathepsin B with the cell surface of human colon cancer cells. Furthermore, we show that the association of cathepsin B with caveolae is regulated by the activation of K-*ras*.

Multiple genetic alterations have been associated with colorectal tumorigenesis in humans including the activation of the K-*ras* protooncogene [49, 50]. The disruption in the mutant K-*ras* allele in HKh-2 cells caused a loss in their capacity for anchorage-independent growth and tumorigenicity in nude mice compared to HCT 116 cells [26,51]. In the present study, we observed differences in cathepsin B expression, secretion, and activity between HCT 116 and HKh-2 cells. The intracellular steady-state level of cathepsin B was lower in HCT 116 cells compared to HKh-2 cells, a finding consistent with HCT 116 cells secreting higher levels of cathepsin B and exhibiting a higher percentage of pericellular cathepsin B activity than did HKh-2 cells. Thus, active K-ras appears to modulate cathepsin B trafficking and secretion in these cells. A functional role for ras in cathepsin B distribution has already been established in breast cancer [52], melanoma [53], and osteoclast [54] cell lines. Mutations in K-*ras* have been correlated to an upregulation in cathepsin B expression and activity in colorectal carcinoma cell lines

[55] and primary human colorectal carcinomas [56]. In addition, Kim et al. [56] reported that a mutation in K-*ras* or an expression of altered forms of N-ras protein increases the tumorigenicity of colorectal carcinomas by inducing the expression of both cathepsin B and cathepsin L. Expression and activity of mature cathepsin B on the plasma membrane of H-*ras*–transformed MCF-10 breast epithelial cells also have been shown to be upregulated without alterations in cathepsin B mRNA levels [23]. Thus, modulation of K-ras and H-ras expression appears to increase the trafficking of active cathepsin B to the cell surface, which in turn contributes to the invasive potential of these cells. A recent study from our laboratory using Matrigel (BD Biosciences, San Diego, CA) invasion assays confirmed that HCT 116 cells are more invasive than HKh-2 cells, and inhibitor studies indicated that cathepsin B is involved in this invasion [13]. Our current data also show that the activation of K-*ras* in HCT 116 cells increases the expression of caveolin-1, the major structural protein of caveolae, and p11, a binding partner for cathepsin B. We hypothesize that in these colon cancer cells, the modulation of caveolin-1 and p11 expression by active K-ras may regulate the increase in cathepsin B trafficking to, and activity at, the cell surface.

Upregulation of p11 has been linked to tumorigenicity and malignancy of various cell lines [42,57]. On the other hand, the role of caveolin-1 in tumor cells remains controversial. The *caveolin-1* gene is located on human chromosome 7q31.1 [58], a region frequently deleted in human breast cancer [59]. Caveolin-1 was identified as one of 26 gene products that are downregulated in breast cancer cells and, as such, has been suggested to be a potential tumor suppressor [60]. Evidence also shows that the transformation of NIH 3T3 fibroblasts with activated v-*abl* or H-*ras* reduces caveolin-1 expression, which in turn leads to the loss of anchorage-dependent growth and the ability of these cells to form foci on soft agar [61]. Nonetheless, several observations argue against caveolin-1 as a tumor suppressor. Our current data demonstrate that the expression of caveolin-1 is upregulated in the more invasive HCT 116 colon cancer cells. Caveolin-1 overexpression is seen in primary and metastatic prostate carcinomas [62,63], invasive ductal breast carcinomas [62], high-grade bladder

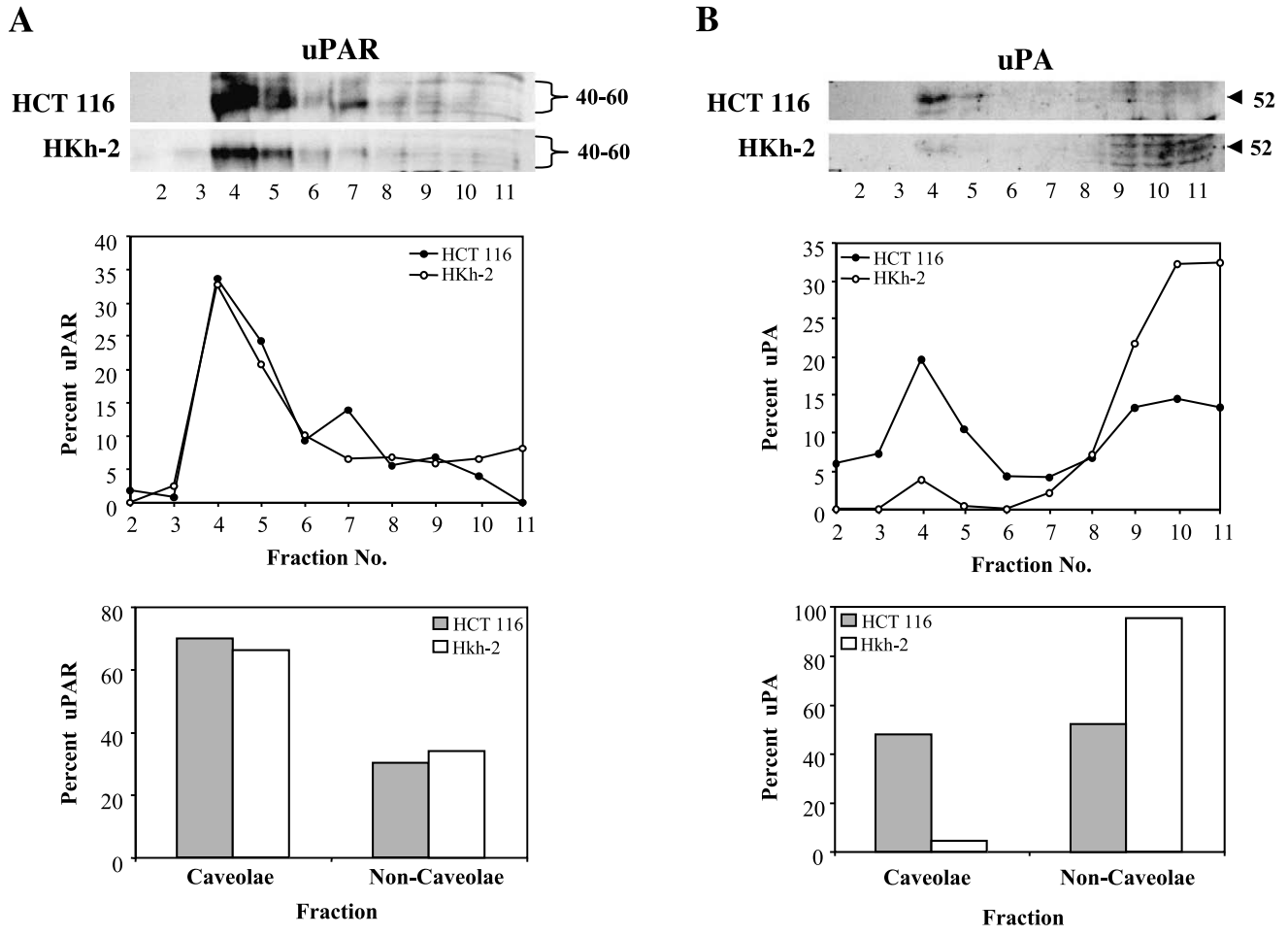

Figure 6. *Identification of uPA and uPAR in caveolae of human colorectal carcinoma cells. Equal amounts of protein for HCT 116 and HKh-2 cells were subjected to subcellular fractionation on a sucrose gradient after homogenization in sodium carbonate buffer, pH 11.0 (see Materials and Methods section). Fractions were collected from the top of the gradient and equal volume aliquots were analyzed by SDS-PAGE and immunoblotted for anti–human uPAR (A) and anti–human uPA (B). Densitometric analysis of the uPAR and uPA protein bands from HCT 116 and HKh-2 fractions was performed and presented as percent uPAR and uPA in individual fractions as a function of the total (sum of fractions 2–11) and percent uPAR and uPA distributed into two major fractions: caveolae (sum of fractions 2–6) and noncaveolae (sum of fractions 7–11).*

cancers [64], and advanced-stage ovarian tumors [65]. Moreover, a positive correlation has been observed between caveolin-1 and caveolae expression and multidrug resistance of colon, breast, ovarian, and lung cancer cell lines [66–68]. In colon and prostate cancers, upregulation of caveolin-1 is believed to contribute to their invasive potential [69,70]. A study by Fine et al. [69] revealed that the expression of caveolin-1 is elevated in colon adenocarcinomas in comparison to normal colonic epithelium and adenomas. In addition, they reported a more diffuse cytoplasmic staining pattern for caveolin-1 in these tumor cells instead of the typical membranous pattern, thus suggesting alterations in the intracellular trafficking of caveolin-1. Although studies by Bender et al. [67] reported higher levels of caveolin-1 in normal colon tissues compared to colon carcinoma cell lines, they did suggest that the initial downregulation of caveolin-1 in colon cancer cells may be reversible because they observed an upregulation of caveolin-1 in metastatic colon carcinoma cells in comparison to their parental counterparts. Such results imply a dual role for caveolin-1: one as a tumor suppressor during early tumor development, and another as a tumor promoter during late-stage tumorigenesis and metastasis.

During the progression of colon cancer, active cathepsin B is redistributed to the basal plasma membrane, and expression of the enzyme is associated with a shortened survival [20,21]. The present study is the first to identify caveolae as a site for association of active cathepsin B with the cell surface of colorectal carcinoma cells. Caveolae are highly lipid-rich subdomains of the plasma membrane that are believed to play roles in endocytosis, cholesterol transport, and cell signaling events [71]. More recently, caveolae have been linked to cell surface proteolysis. The colocalization of MMP-2, its activator MT1-MMP, a proposed receptor $\alpha v\beta_3$, and the inhibitor TIMP-2 with caveolin-1 implicates caveolae as a site to restrict proteolysis of the matrix to a limited microenvironment at the cell surface [29,30]. In addition, the clustering of uPAR and its ligand uPA in caveolae has been shown to enhance the activation of plasminogen at the cell surface [28], a process that is also involved in cell invasion. Although uPA and uPAR have previously been detected on the surface of HCT 116 cells [35], in the present study, we identify these proteins specifically in caveolae of these cells. The localization of uPA, uPAR, and cathepsin B to caveolae of HCT 116 cells is interesting as cathepsin B has been reported to activate both soluble and membrane-bound pro-uPA [15–17]—an early event associated with proteolytic cascades involved in tumor invasion. Studies conducted in our laboratory using a novel confocal assay showed pericellular degradation of quenched fluorescent type IV collagen (DQ collagen IV) by living BT20 breast cancer cells [12]—a degradation that involves a cascade of proteolytic enzymes including cathepsin B, plasminogen cascade serine proteases, and MMPs. These assays have also been performed using living HCT 116 and HKh-2 cells and show enhanced pericellular degradation of DQ collagen IV by HCT 116 cells—degradation that can be reduced by protease inhibitors [13]. Increased expression of uPAR on the surface of HCT 116 cells compared to HKh-2 cells has also been shown to contribute to increased laminin degradation by these cells [35]. The fact that active cathepsin B, uPA, and uPAR were detected in the caveolae of HCT 116 cells suggests a functional role for caveolae-associated cathepsin B in tumor cell invasion of colorectal carcinoma cells, possibly in coordination with the uPA/uPAR system and MMPs.

The mechanism(s) by which cathepsin B binds to the extracellular surface of tumor cells currently remains unknown. Procathepsin B was found to bind directly to p11, and mature single-chain and double-chain forms of cathepsin B were also found in membrane extracts that contain both the light and heavy chains of AIIt [34]. Previous reports have shown colocalization of p36 and p11 in the caveolae of various cell lines including endothelial and MDCK cells [31,32]. We also detected p11 and p36 in the caveolae of HCT 116 cells, thus strongly implicating AIIt as a potential binding protein for caveolae-associated cathepsin B in these cells. As a membrane protein, AIIt is believed to act as a receptor for many different ligands such as the ECM proteins collagen I and tenascin C, as well as proteases including plasmin(ogen), tPA, and cathepsin B (for review, see Ref. [72]). Both p36 [73] and p11 [74] were shown to bind plasminogen and stimulate its activation via a tPA-dependent event, resulting in cell surface matrix degradation and invasion through the ECM [75]. In tumor cells, the AIIt-dependent associations between ECM proteins and enzymes that degrade them appear to facilitate a regulated modification and turnover of the ECM, essential for tumor invasion. In support of this hypothesis, Choi et al. [42] have demonstrated that upregulating the expression of p11 in HT1080 fibrosarcoma cells increases plasmin production and invasiveness. Our data show that activation of K-*ras* upregulates the expression of p11 and the distribution of p11 to caveolae of colon cancer cells. The expression of p11 in caveolae of HCT 116 cells appears to correlate with an increase in trafficking of cathepsin B and uPA to caveolae of these cells. Thus, we suggest that the presence of p11 as a binding partner for cathepsin B in the caveolae may serve to increase the interaction between cathepsin B and uPA/uPAR, and thus initiate proteolytic cascades involved in tumor cell invasion. Future experiments, however, will be required to elucidate the mechanism(s) for and functional consequences of cathepsin B trafficking to the caveolae.

References

[1] Liotta LA, Rao CN, and Barsky SH (1983). Tumor invasion and the extracellular matrix. *Lab Invest* **49,** 636–49.

[2] McCawley LJ, and Matrisian LM (2001). Tumor progression: defining the soil round the tumor seed. *Curr Biol* **11,** R25–R37.

[3] Mignatti P, Robbins E, and Rifkin DB (1986). Tumor invasion through the human amniotic membrane: requirement for a proteinase cascade. *Cell* **47,** 487–98.

[4] Koblinski JE, Ahram M, and Sloane BF (2000). Unraveling the role of proteases in cancer. *Clin Chim Acta* **291,** 113–35.

[5] Nishimura Y, Kawabata T, and Kato K (1988). Identification of latent procathepsins B and L in microsomal lumen: characterization of enzymatic activation and proteolytic processing *in vitro. Arch Biochem Biophys* **261,** 64–71.

[6] Mort JS, and Buttle DJ (1997). Cathepsin B. *Int J Biochem Cell Biol* **29,** 715–20.

[7] Buck MR, Karustis DG, Day NA, Honn KV, and Sloane BF (1992). Degradation of extracellular-matrix proteins by human cathepsin B from normal and tumour tissues. *Biochem J* **282,** 273–78.

[8] Rozhin J, Robinson D, Stevens MA, Lah TT, Honn KV, Ryan RE, and Sloane BF (1987). Properties of a plasma membrane–associated cathepsin B–like cysteine proteinase in metastatic melanoma variants. *Cancer Res* **47,** 6620–628.

[9] Rozhin J, Sameni M, Ziegler G, and Sloane BF (1994). Pericellular pH affects distribution and secretion of cathepsin B in malignant cells. *Cancer Res* **54,** 6517–525.

[10] Linebaugh BE, Sameni M, Day NA, Sloane BF, and Keppler D (1999). Exocytosis of active cathepsin B enzyme activity at pH 7.0, inhibition and molecular mass. *Eur J Biochem* **264,** 100–109.

[11] Brix K, Linke M, Tepel C, and Herzog V (2001). Cysteine proteinases mediate extracellular prohormone processing in the thyroid. *Biol Chem* **382,** 717–25.

[12] Sameni M, Moin K, and Sloane BF (2000). Imaging proteolysis by living human breast cancer cells. *Neoplasia* **2,** 496–504.

[13] Sameni M, Dosescu J, Moin K, and Sloane BF (2003). Functional imaging of proteolysis: stromal and inflammatory cells increase tumor proteolysis. *Mol Imaging* **2,** 1–17.

[14] Sameni M, Dosescu J, and Sloane BF (2001). Imaging proteolysis by living human glioma cells. *Biol Chem* **382,** 785–88.

[15] Kobayashi H, Moniwa N, Sugimura M, Shinohara H, Ohi H, and Terao T (1993). Increased cell-surface urokinase in advanced ovarian cancer. *Jpn J Cancer Res* **84,** 633–40.

[16] Ikeda Y, Ikata T, Mishiro T, Nakano S, Ikebe M, and Yasuoka S (2000). Cathepsins B and L in synovial fluids from patients with rheumatoid arthritis and the effect of cathepsin B on the activation of pro-urokinase. *J Med Invest* **47,** 61–75.

[17] Guo M, Mathieu PA, Linebaugh B, Sloane BF, Reiners Jr, JJ 2002. Phorbol ester activation of a proteolytic cascade capable of activating latent TGF-β: a process initiated by the exocytosis of cathepsin B. *J Biol Chem* **277,** 14829–837.

[18] Zavadil J, Bitzer M, Liang D, Yang YC, Massimi A, Kneitz S, Piek E, and Bottinger EP (2001). Genetic programs of epithelial cell plasticity directed by transforming growth factor-beta. *Proc Natl Acad Sci USA* **98,** 6686–691.

[19] Yan Z, Kim GY, Deng X, and Friedman E (2002). Transforming growth factor beta 1 induces proliferation in colon carcinoma cells by Ras-dependent, smad-independent down-regulation of p21cip1. *J Biol Chem* **277,** 9870–879.

[20] Campo E, Munoz J, Miquel R, Palacin A, Cardesa A, Sloane BF, and Emmert-Buck MR (1994). Cathepsin B expression in colorectal carcinomas correlates with tumor progression and shortened patient survival. *Am J Pathol* **145,** 301–309.

[21] Hazen LG, Bleeker FE, Lauritzen B, Bahns S, Song J, Jonker A, Van Driel BE, Lyon H, Hansen U, Kohler A, and Van Noorden CJ (2000). Comparative localization of cathepsin B protein and activity in colorectal cancer. *J Histochem Cytochem* **48,** 1421–430.

[22] Fearon E, and Vogelstein B (1990). A genetic model for colorectal tumorigenesis. *Cell* **61,** 759–67.

[23] Sloane BF, Moin K, Sameni M, Tait LR, Rozhin J, and Ziegler G (1994). Membrane association of cathepsin B can be induced by transfection of human breast epithelial cells with c-Ha-*ras* oncogene. *J Cell Sci* **107,** 373–84.

[24] Marten K, Bremer C, Khazaie K, Sameni M, Sloane BF, Tung CH, and Weissleder R (2002). Detection of dysplastic intestinal adenomas using enzyme sensing molecular beacons in mice. *Gastroenterology* **122,** 406–14.

[25] Dove WF, Gould KA, Luongo C, Moser AR, and Shoemaker AR (1995). Emergent issues in the genetics of intestinal neoplasia. *Cancer Surv* **25,** 335–55.

[26] Shirasawa S, Furuse M, Yokoyama N, and Sasazuki T (1993). Altered growth of human colon cancer cell lines disrupted at activated Ki-*ras*. *Science* **260,** 85–88.

[27] White MA, and Anderson RG (2001). Which *Ras* rides the raft? *Nat Cell Biol* **3,** E172.

[28] Stahl A, and Mueller BM (1995). The urokinase-type plasminogen activator receptor, a GPI-linked protein, is localized in caveolae. *J Cell Biol* **129,** 335–44.

[29] Annabi B, Lachambre M, Bousquet-Gagnon N, Page M, Gingras D, and Beliveau R (2001). Localization of membrane-type 1 matrix metalloproteinase in caveolae membrane domains. *Biochem J* **353,** 547–53.

[30] Puyraimond A, Fridman R, Lemesle M, Arbeille B, and Menashi S (2001). MMP-2 colocalizes with caveolae on the surface of endothelial cells. *Exp Cell Res* **262,** 28–36.

[31] Sargiacomo M, Sudol M, Tang Z, and Lisanti MP (1993). Signal transducing molecules and glycosyl-phosphatidylinositol–linked proteins form a caveolin-rich insoluble complex in MDCK cells. *J Cell Biol* **122,** 789–807.

[32] Harder T, and Gerke V (1994). The annexin II2p11(2) complex is the major protein component of the Triton X-100–insoluble low-density fraction prepared from MDCK cells in the presence of Ca^{2+}. *Biochem Biophys Acta* **1223,** 375–82.

[33] Kim J, and Hajjar KA (2002). Annexin II: a plasminogen–plasminogen activator co-receptor. *Front Biosci* **7,** 341–48.

[34] Mai J, Finley Jr, RL, Waisman DM, and Sloane BF 2000. Human procathepsin B interacts with the annexin II tetramer on the surface of tumor cells. *J Biol Chem* **275,** 12806–812.

[35] Allgayer H, Wang H, Shirasawa S, Sasazuki T, and Boyd D (1999). Targeted disruption of the K-*Ras* oncogene in an invasive colon cancer cell line down-regulated urokinase receptor expression and plasminogen dependent proteolysis. *Br J Cancer* **80,** 1884–891.

[36] Moin K, Day NA, Sameni M, Hasnain S, Hirama T, and Sloane BF (1992). Human tumour cathepsin B. Comparison with normal liver cathepsin B. *Biochem J* **285,** 427–34.

[37] Song KS, Li S, Okamoto T, Quilliam LA, Sargiacomo M, and Lisanti MP (1996). Co-purification and direct interaction of *Ras* with caveolin, an integral membrane protein of caveolae microdomains. Detergent-free purification of caveolae microdomains. *J Biol Chem* **271,** 9690–697.

[38] Smart EJ, Ying Y, Mineo C, and Anderson RG (1995). A detergent-free method for purifying caveolae membrane from tissue culture cells. *Proc Natl Acad Sci USA* **92,** 10104–108.

[39] Willingham MC (1990). Immunocytochemical methods: useful and informative tools for screening hybridomas and evaluating antigen expression. *Focus* **12,** 62–67.

[40] Murata M, Miyashita S, Yokoo C, Tamai M, Hanada K, Hatayama K, Towatari T, Nikawa T, and Katunuma N (1991). Novel epoxysuccinyl peptides. Selective inhibitors of cathepsin B, *in vitro*. *FEBS Lett* **280,** 307–10.

[41] Waisman D (1995). Annexin II tetramer: structure and function. *Mol Cell Biochem* **149** (150), 301–22.

[42] Choi KS, Fogg DK, Yoon CS, and Waisman DM (2003). p11 regulates extracellular plasmin production and invasiveness of HT1080 fibrosarcoma cells. *FASEB J* **17,** 235–46.

[43] Kassam G, Choi KS, Ghuman J, Kang HM, Fitzpatrick SL, Zackson T, Zackson S, Toba M, Shinomiya A, and Waisman DM (1998). The role of annexin II tetramer in the activation of plasminogen. *J Biol Chem* **273,** 4790–799.

[44] Lisanti MP, Scherer PE, Vidugiriene J, Tang Z, Hermanowski-Vosatka YH, Tu YH, Cook RF, and Sargiacomo M (1994). Characterization of caveolin-rich membrane domains isolated from an endothelial-rich source: implications for human disease. *J Cell Biol* **126,** 111–26.

[45] Scherer PE, Tang Z, Chun M, Sargiacomo M, Lodish H, and Lisanti MP (1995). Caveolin isoforms differ in their N-terminal protein sequence and subcellular distribution. Identification and epitope mapping of an isoform-specific monoclonal antibody probe. *J Biol Chem* **270,** 16395–401.

[46] Wei Y, Yang X, Liu Q, Wilkins JA, and Chapman HA (1999). A role for caveolin and the urokinase receptor in integrin-mediated adhesion and signaling. *J Cell Biol* **144,** 1285–294.

[47] Schwab W, Gavlik JM, Beichler T, Funk RH, Albrecht S, Magdolen V, Luther T, Kasper M, and Shakibaei M (2001). Expression of the urokinase-type plasminogen activator receptor in human articular chondrocytes: association with caveolin and beta 1-integrin. *Histochem Cell Biol* **115,** 317–23.

[48] Cavallo-Medved D, and Sloane BF (2003). Cell surface cathepsin B: understanding its functional significance. In Zucker S, Chen W-T (Eds.), Cell Surface Proteases, pp. 313–41 Elsevier, USA.

[49] Bos JL, Verlaan-de Vries M, Marshall CJ, Veeneman GH, van Boom AJ, and van der Eb AJ (1986). A human gastric carcinoma contains a single mutated and an amplified normal allele of the Ki-*ras* oncogene. *Nucleic Acids Res* **14,** 1209–217.

[50] Bos JL, Fearon ER, Hamilton SR, Verlaan-de Vries M, van Boom JH, van der Eb AJ, and Vogelstein B (1987). Prevalence of *ras* gene mutations in human colorectal cancers. *Nature* **327,** 293–97.

[51] Okada F, Rak JW, Croix BS, Lieubeau B, Kaya M, Roncari L, Shirasawa T, Sasazuki T, and Kerbel RS (1998). Impact of oncogenes in tumor angiogenesis: mutant K-*ras* up-regulation of vascular endothelial growth

factor/vascular permeability factor is necessary, but not sufficient for tumorigenicity of human colorectal carcinoma cells. *Proc Natl Acad Sci USA* **95,** 3609–614.

[52] Premzl A, Zavasnik-Bergant V, Turk V, and Kos J (2003). Intracellular and extracellular cathepsin B facilitate invasion of MCF-10A neoT cells through reconstituted extracellular matrix *in vitro*. *Exp Cell Res* **283,** 206–14.

[53] Donatien PD, Diment SL, Boissy RE, and Orlow SJ (1996). Melanosomal and lysosomal alterations in murine melanocytes following transfection with the v-*ras*-Ha oncogene. *Int J Cancer* **66,** 557–63.

[54] Pascoe D, and Oursler MJ (2001). The Src signaling pathway regulates osteoclast lysosomal enzyme secretion and is rapidly modulated by estrogen. *J Bone Miner Res* **16,** 1028–1036.

[55] Yan Z, Deng X, Chen M, Xu Y, Ahram M, Sloane BF, and Friedman E (1997). Oncogenic c-Ki-*ras* but not oncogenic c-Ha-*ras* up-regulates CEA expression and disrupts basolateral polarity in colon epithelial cells. *J Biol Chem* **272,** 27902–907.

[56] Kim K, Cai J, Shuja S, Kuo T, and Murnane MJ (1998). Presence of activated *ras* correlates with increased cysteine proteinase activities in human colorectal carcinomas. *Int J Cancer* **9,** 324–33.

[57] Yeatman TJ, Updyke TV, Kaetzel MA, Dedman JR, and Nicolson GL (1993). Expression of annexins on the surfaces of non-metastatic and metastatic human and rodent tumor cells. *Clin Exp Metastasis* **11,** 37–44.

[58] Engelman JA, Wykoff CC, Yasuhara S, Song KS, Okamoto T, and Lisanti MP (1997). Recombinant expression of caveolin-1 in oncogenically transformed cells abrogates anchorage-independent growth. *J Biol Chem* **272,** 16374–381.

[59] Zenklusen JC, Thompson JC, Troncoso P, Kagan J, and Conti CJ (1994). Loss of heterozygosity in human primary prostate carcinomas: a possible tumor suppressor gene at 7q31.1. *Cancer Res* **54,** 6370–373.

[60] Sager R, Sheng S, Anisowicz A, Sotiropoulou G, Zou Z, Stenman G, Swisshelm K, Chen Z, Hendrix MJ, and Pemberton P (1994). RNA genetics of breast cancer: maspin as paradigm. *Cold Spring Harb Symp Quant Biol* **59,** 537–46.

[61] Koleske AJ, Baltimore D, and Lisanti MP (1995). Reduction of caveolin and caveolae in oncogenically transformed cells. *Proc Natl Acad Sci USA* **92,** 1381–385.

[62] Yang G, Truong LD, Timme TL, Ren C, Wheeler TM, Park SH, Nasu Y, Bangma CH, Kattan MW, Scardino PT, and Thompson TC (1998). Elevated expression of caveolin is associated with prostate and breast cancer. *Clin Cancer Res* **4,** 1873–880.

[63] Yang G, Truong LD, Wheeler TM, and Thompson TC (1999). Caveolin-1 expression in clinically confined human prostate cancer: a novel prognostic marker. *Cancer Res* **59,** 5719–723.

[64] Rajjayabun PH, Garg S, Durkan GC, Charlton R, Robinson MC, and Mellon JK (2001). Caveolin-1 expression is associated with high-grade bladder cancer. *Urology* **58,** 811–14.

[65] Davidson B, Nesland JM, Goldberg I, Kopolovic J, Gotlieb WH, Bryne G, Ben-Baruch G, Berner A, and Reich R (2001). Caveolin-1 expression in advanced-stage ovarian carcinoma—a clinicopathologic study. *Gynecol Oncol* **81,** 166–71.

[66] Lavie Y, Fiucci G, and Liscovitch M (1998). Up-regulation of caveolae and caveolar constituents in multidrug-resistant cancer cells. *Biol Chem* **273,** 32380–383.

[67] Bender FC, Reymond MA, Bron C, and Quest AF (2000). Caveolin-1 levels are down-regulated in human colon tumors, and ectopic expression of caveolin-1 in colon carcinoma cell lines reduces cell tumorigenicity. *Cancer Res* **60,** 5870–878.

[68] Yang C-PH, Galbiati F, Volonte D, Horwitz SB, and Lisanti MP (1998). Upregulation of and caveolin-1 caveolae organelles in Taxol-resistant A549 cells. *FEBS Lett* **439,** 368–72.

[69] Fine SW, Lisanti MP, Galbiati F, and Li M (2001). Elevated expression of caveolin-1 in adenocarcinoma of the colon. *Am J Clin Pathol* **115,** 719–24.

[70] Tahir SA, Yang G, Ebara S, Timme TL, Satoh T, Li L, Goltsov A, Ittmann M, Morrisett JD, and Thompson TC (2001). Secreted caveolin-1 stimulates cell survival/clonal growth and contributes to metastasis in androgen-insensitive prostate cancer. *Cancer Res* **61,** 3882–885.

[71] Smart EJ, Graf GA, McNiven MA, Sessa WC, Engelman JA, Scherer T, Okamoto T, and Lisanti MP (1999). Caveolins, liquid-ordered domains, and signal transduction. *Mol Cell Biol* **19,** 7289–304.

[72] Mai J, Waisman DM, and Sloane BF (2000). Cell surface complex of cathepsin B/annexin II tetramer in malignant progression. *Biochim Biophys Acta* **36072,** 1–16.

[73] Hajjar KA, and Hamel NM (1990). Identification and characterization of human endothelial cell membrane binding sites for tissue plasminogen activator and urokinase. *J Biol Chem* **265,** 2908–916.

[74] Kassam G, Le BH, Choi KS, Kang HM, Fitzpatrick SL, Louie P, and Waisman DM (1998). Plasminogen-mediated matrix invasion and degradation by macrophages is dependent on surface expression of annexin II. *Biochemistry* **37,** 16958–966.

[75] Falcone DJ, Borth W, Khan KM, and Hajjar KA (2001). Plasminogen-mediated matrix invasion and degradation by macrophages is dependent on surface expression of annexin II. *Blood* **97,** 777–84.